UNIVERSIDADE D COIMBRA FACULDADE DE MEDICINA

MESTRADO INTEGRADO EM MEDICINA – TRABALHO FINAL

ANDRÉ SANTOS PAULA

Usher syndrome: dysfunctional olfactory brain regions and statistical classification of disease status using fMRI

ARTIGO CIENTÍFICO

ÁREA CIENTÍFICA DE NEUROLOGIA

Trabalho realizado sob a orientação de:

PROFESSOR DOUTOR MIGUEL CASTELO-BRANCO

MESTRE ISABEL CATARINA DUARTE

ABRIL 2019

USHER SYNDROME: DYSFUNCTIONAL OLFACTORY BRAIN REGIONS AND STATISTICAL CLASSIFICATION OF DISEASE STATUS USING FMRI

André Santos Paula[1], Sónia Ferreira[2], Andreia Pereira[2], João Carlos Ribeiro[2,3], Eduardo Duarte Silva[2], Isabel Catarina Duarte[4], Miguel Castelo-Branco[1,4]

[1]Faculty of Medicine, University of Coimbra, Portugal

[2]Institute for Biomedical Imaging and Life Sciences, Faculty of Medicine, University of Coimbra, Portugal

[3]Otolaryngology Unit, Centro Hospitalar e Universitário de Coimbra (CHUC), Portugal

[4]Institute of Nuclear Sciences Applied to Health, University of Coimbra, Portugal

TABLE OF CONTENTS

ABSTRACT

BACKGROUND

Usher syndrome (USH) is a rare autosomal recessive disease, affecting vision and audition, and showing clinical and genetic heterogeneity. Evidence of olfactory impairment in USH patients has emerged through psychophysical and structural imaging studies. However, the effect of this condition in the central olfactory processing network has not yet been evaluated through functional imaging studies. We sought to compare olfactory task-related activity in the orbitofrontal (OFC) and piriform (PC) cortices between USH patients and healthy subjects. Also, a classification analysis between these groups was carried out to assess functional imaging potential of discriminating USH patients.

MATERIALS AND METHODS

Twenty-six age- and gender-matched controls with no history of olfactory dysfunction and 27 USH patients (4 USH1, 21 USH2, 2 USH3) were studied. Functional magnetic resonance imaging (fMRI) was used with an olfactory detection task to evaluate responses in the OFC and PC. Four butanol concentration levels were presented to each participant. These regions were functionally defined using an automated meta-analysis toolbox, Neurosynth. In the univariate analyses a multi-subject general linear model (GLM) with random effects was performed and the beta estimates from each region were used to compare between groups. In the classification analysis a separate-subject GLM was performed and t-statistic maps were created for each subject which then were used as input to a logistic regression classifier.

RESULTS

An interaction effect between group and butanol level was found in the right OFC ($F(2.365;118.247)=3.032$, $p=0.043$). Also, an interaction effect between group and butanol level emerged in the right PC ($F(3,150)=4.537$, $p=0.004$). Stimulus-evoked activation in both the left OFC and left PC did not show any significant effect. Planned contrast of the highest odor concentration minus the lowest odor concentration activation between groups revealed a significant difference in the right OFC ($t(51)=2.339$, $p=0.023$). The same contrast showed a significant difference between USH patients and controls in the right PC ($t(51)=-3.380$, $p=0.001$).

As for the USH patients vs controls classification analysis we report a predictor model with accuracy of 71.7% ($p=0.0072$), sensitivity of 67.7% ($p=0.0328$), specificity of 77.3% ($p=0.0041$) and an AUC of 0.785 ($p=0.0087$).

CONCLUSION

These data provide evidence of decreased activation in the right PC and increased compensatory activation in the right OFC in USH patients reinforcing the notion of dysfunctional olfactory sensory function. Also, it shows that olfactory fMRI patterns can discriminate USH patients from controls which holds promise in USH diagnosis improvement.

KEYWORDS: Usher Syndrome; Smell; Odor; Functional Magnetic Resonance Imaging; Multivariate Pattern Analysis.

ABBREVIATIONS

BA – Brodmann

fMRI – Functional magnetic resonance imaging

GLM – General linear model

MVPA – Multivariate pattern analysis

OFC – Orbitofrontal cortex

PC – Piriform cortex

ROI – Region-of-interest

RP – Retinitis pigmentosa

USH – Usher syndrome

USH1 – Usher syndrome type 1

USH2 – Usher syndrome type 2

USH3 – Usher syndrome type 3

INTRODUCTION

Usher syndrome (USH) is a rare autosomal recessive disease whose clinical manifestations are heterogeneous and severely debilitating. It is the most common genetic cause of deaf-blindness and is incurable. Typical manifestations include retinitis pigmentosa (RP), hearing loss and vestibular dysfunction. This condition is classified into three clinical types (type I, II and III) according to the clinical presentation. Type I USH (USH1) is characterized by severe to profound congenital deafness, vestibular areflexia and rapid onset of RP. Type II USH (USH2) clinical presentation includes moderate to severe hearing loss, normal vestibular function and late onset of RP. Type III USH (USH3) patients suffer from progressive hearing loss, sporadic vestibular dysfunction and variable onset of RP (1).

It has been demonstrated that the pathophysiology of USH is related to photoreceptor cells degeneration in the retina and dysfunctional cilia motility of hair cells in the cochlea and vestibular labyrinth (2,3). There are 12 genetic loci known to be involved in this disease: *USH1B-H*, *USH2A*, *C-D* and *USH3A-B*. These genes encode proteins involved in cell adherence, protein scaffolding and signaling processes. Mutations within any of these genetic loci results in functional impairment of key proteins of cochlear and photoreceptor cells (4). Thus, USH can be broadly viewed as a sensory ciliopathy.

Since olfactory receptor cells are ciliated, it has been hypothesized that these patients could also exhibit olfactory loss (5). In fact, olfactory deficits have already been reported not only in mice models of this syndrome (6) but also in USH patients (5). Recently, a larger clinical study showed that USH1 patients exhibit a faster ageing olfactory decline when compared to healthy individuals (7). Furthermore, it has been demonstrated that the olfactory sulcus depth is reduced in USH patients and the olfactory threshold is negatively correlated with olfactory bulb volume in USH1 patients (8). However, the effect of this condition in the central olfactory processing network remains to be evaluated through functional imaging studies.

Olfactory processing begins with the interaction between a molecular stimulus and the olfactory receptor neurons. The axons of olfactory receptor neurons (first-order neurons) synapse onto apical dendrites of olfactory bulb neurons (second-order neurons). Axons from the latter leave the bulb in the olfactory tract and project to the primary olfactory cortex. This region is mainly comprised by the piriform cortex, rostral entorhinal cortex and the amygdala, which then project to higher-order brain regions such as orbitofrontal cortex, cingulate cortex and insula (9,10).

Some functional magnetic resonance imaging (fMRI) studies have reported diminished activation levels in central olfactory brain regions in anosmia and hyposmia conditions (11,12). Notably, it has been reported that after a 7-day olfactory deprivation there

is a reversible increase in stimulus-evoked activity in orbitofrontal cortex (OFC) and the opposite in the piriform cortex (PC) (13). Thus, it is tempting to speculate that similar alterations may be found in USH patients due to the dysfunctional ciliated olfactory receptor cells.

Several neurological and psychiatric diseases including autistic spectrum disorders (14), social anxiety disorder (15), schizophrenia (16) and major depressive disorder (17) have been investigated through multivariate pattern analysis (MVPA) showing that it is possible to discriminate patients from healthy subjects based on fMRI activation patterns. Although these studies and classification techniques need further validation, they represent a promising tool in the diagnosis of clinically challenging diseases.

The aim of this work is to study USH olfactory impairment through fMRI by generating stimulus-response curves for functionally-defined regions-of-interest (ROIs) in central olfactory brain areas specifically the piriform cortex and the orbitofrontal cortex. Both univariate and MVPA analysis will be conducted to identify and characterize putative differences between USH patients and controls regarding fMRI activity. In sum, we intend to test two hypotheses: USH patients show different responses in central olfactory areas when compared to healthy individuals and it is possible to discriminate between these two groups using fMRI activity patterns.

MATERIALS AND METHODS

SUBJECTS

Twenty-seven USH patients (19 male and 8 female; mean age=47.41 with SD=12.28) were included in this study. Of these there were 4 USH1, 21 USH2 and 2 USH3. Comparatively, 26 age- and sex-matched controls (18 male and 8 female; mean age=46.42 with SD=12.15) with no history of olfactory dysfunction were also included in this study.

The study was conducted in accordance with the Declaration of Helsinki and was approved by the Ethics Commission of Faculty of Medicine of University of Coimbra. All participants signed a written informed consent after full explanation of research procedures.

All USH patients were diagnosed according to clinical criteria based mainly on ophthalmological and otorhinolaryngological tests by two experienced physicians (18). Genetic tests were later used to confirm the diagnosis.

Both controls and USH patients were subjected to a thorough clinical examination and extensive review of clinical history in order to assess possible confounding factors for olfactory function and fMRI activity responses. Exclusion criteria for this study were visual, olfactory and auditory alterations in controls (2 controls excluded), controls with smoking habits as these are known to have lower olfactory acuity (19) and concomitant pathologies that might affect olfaction such as post-traumatic olfactory dysfunction and post-upper respiratory tract infection (1 control excluded). Abnormal neuroradiological findings (4 patients and 2 controls excluded) and incorrect task execution during fMRI scans (5 patients excluded) were also exclusion factors. USH patients were subjected to Montreal Cognitive Assessment test (MoCA) in order to exclude dementia that is known to potentially cause olfactory impairment (20).

FMRI ACQUISITION

Scanning was performed in a 3-Tesla scanner (Magneton TrioTim, Siemens AG, Germany) at the Portuguese Brain Imaging Network, using a 12-channel birdcage head coil. Two T1-weighted Magnetization-Prepared Rapid Acquisition with Gradient Echo (MPRAGE) sequences (1x1x1 mm^3 voxel size; Repetition Time (TR) 2.53 s; Echo Time (TE) 3.42 ms; Flip Angle (FA) 7º; Field of View (FOV) 256x256 mm^2; 176 slices) were acquired from each participant. Functional sequences (single shot Echo Planar Imaging [EPI]) were acquired 30 deg in the axial plane orthogonal to the Anterior Commissure-Posterior Commissure plane (AC-PC) covering the whole brain (3x3x3 mm^3 voxel size; TR 3s; TE 30 ms; FA 90º, FOV 256x256 mm^2; 43 slices; 86x86 imaging matrix). This slice orientation was chosen to minimize signal dropout in the orbitofrontal and medial temporal areas caused by

susceptibility artifacts as previously described (21). Each functional sequence was preceded by a multi-echo EPI (3.7x3.7x3 mm^3 voxel size; TR 0.4 s; TE_1 4.92 ms; TE_2 7.38 ms; FA 60 deg; FOV 235x235 mm^2; 36 slices; 64x64 imaging matrix) acquisition in order to correct for EPI distortion due to susceptibility artifacts.

OLFACTORY THRESHOLDS

Following previous studies (22), each participant performed a butanol olfactory threshold test through a single staircase procedure with a set of 8 solutions ranging from 4% to 0.002% following a 1:3 dilution with water as a solvent. In this context the olfactory threshold is the lowest butanol concentration detected by an individual. The butanol solution was presented to participants birhinally. Butanol is a bimodal odorant activating both the olfactory and trigeminal nerve (12).

OLFACTORY FMRI TASK

A random staircase design with four concentration levels of butanol was implemented. The concentration levels were as follows: the butanol threshold concentration (β_0) determined prior to scanning, one concentration below (β_{-1}), one concentration above (β_{+1}) and two concentrations above (β_{+2}). Participants were instructed to press a button whenever they detected the odorant after the green or white (for patients with severe visual impairment) screen. The first presented concentration was random. Then, whenever the individual detected the odorant, the next concentration was lower. On the other hand, whenever the participant did not detect the stimulus, the next concentration was higher. This approach was used to guarantee an adaptive design. Participants were instructed to breathe normally and not to sniff as sniffing can induce signal change in primary olfactory regions (21). Odorless air was used as baseline. In order to prevent olfactory receptors saturation, a supra-threshold coffee odorant was released three times per run. Odorant release blocks (black screen) lasted 30 s each allowing proper detection in olfactory impaired patients (21). Each run consisted of 18 blocks of odorless air, 3 blocks of coffee and 12 blocks of butanol and thereby lasting 16 min and 30 s. All participants completed two functional runs except 4 patients that only completed one run due to fatigue.

The stimulus was designed using Matlab 2010b (The MathWorks, Inc., USA) with Psychophysics Toolbox 3 extensions and it was presented in a back-projection Liquid Crystal Display monitor (NordicNeuroLab, Norway) with a mirror mounted above the coil. Responses were collected with an fMRI response pad (Lumina LU400-PAIR, Cedrus Corporation, USA). The odorants were presented using an olfactometer (Mag Design and Engineering, Redwood

City, USA) which was controlled using the Matlab script and was kept in the control room. Individual conduits passed to the MRI room through the waveguide and were connected to the individual odorant containers. Nasal cannulae were used to deliver air flow bilaterally.

IMAGE PROCESSING

Image processing was performed using BrainVoyager 20.6.2 (Brain Innovation BV, The Netherlands). The two T1-weighted anatomical images were averaged for each participant, re-oriented in relation to AC-PC and transformed to Talairach (TAL) coordinate system. These images were used to project task-related responses.

Anatabacus, a plugin for BrainVoyager software, was used to correct EPI geometric distortion due to susceptibility artifacts. Preprocessing included scan time correction, temporal high-pass filtering (2 cycles per run), correction for small inter-scan head movements, spatial normalization and spatial smoothing (FWHM 6 mm). Since a strong habituation effect on the hemodynamic response was verified in the second half of the stimulation block our model only accounted for stimulus effects in the first half.

DEFINITION OF ROIS

In order to define functional ROIs, we used the automated meta-analysis toolbox Neurosynth (23) similarly to other studies (24,25). A meta-analysis of 74 studies using the term “olfactory” was retrieved. This meta-analysis provided a reverse-inference z-score map of brain regions related to the olfactory central network (FDR-corrected at $p<0.01$). The map was transformed to TAL coordinate system and was thresholded at a z value of 2.5 and a 50 voxel cluster-threshold. This restricted the map to known olfactory related regions only and eliminated spurious voxels. The resulting map contained 325 voxels (3x3x3 mm^3 voxel size after transformation) (Figure 1). Next, the map was split into several clusters and sub-clusters (local maxima) (Table 1). Bilateral PC and OFC (BA 11) were used as ROIs in the univariate analysis. The left sub-cluster on the fronto-temporal junction which we used as left PC includes a small portion of the left amygdala. In respect to the MVPA analysis all olfactory regions were used except for the lateral globus pallidus which resulted in a 317 voxel-extent olfactory map.

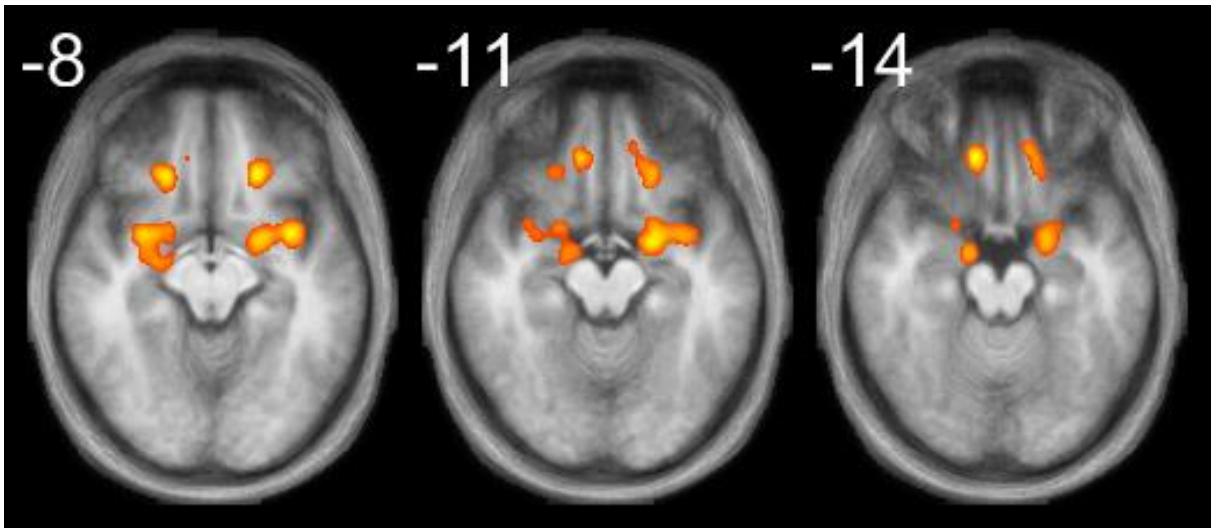

Figure 1: Central olfactory map derived from Neurosynth after transformation to TAL coordinate system. A z value threshold of 2.5 and a 50-voxel cluster threshold was applied. An averaged anatomical image of controls is used to project the statistical map. Left side corresponds to right hemisphere.

Table 1: All regions-of-interest yielded by splitting the olfactory statistical map into sub-clusters. Talairach coordinates.

Region	H	Peak			Voxel Extent
		x	y	z	
OFC (BA 11)	R	12	35	-14	27
OFC (BA 11)	L	-12	38	-14	21
OFC (BA 47)	R	21	26	-8	32
OFC (BA 47)	L	-21	29	-8	41
OFC (BA 47)/temporal pole	R	24	11	-20	11
Piriform cortex	R	15	-7	-14	32
Piriform cortex/amygdala	L	-21	-1	-11	55
Amygdala	R	24	-10	-8	15
Insula	L	-33	2	-8	48
Insula	R	30	2	-8	35
Lateral globus pallidus	R	18	-1	-2	8

H=hemisphere, R=right, L=left, OFC=orbitofrontal cortex, BA=Brodmann area.

UNIVARIATE ANALYSIS

A multi-subject general linear model (GLM) with random effects was performed in BrainVoyager using 5 task-related predictors (coffee, butanol β_{-1}, butanol β_0, butanol β_{+1}, and butanol β_{+2}) and additional predictors accounting for within-run head movement. Beta estimate values for each condition were extracted from each ROI. Statistical analyses were then carried out with IBM SPSS Statistics 22 (IBM Corporation, USA). We performed repeated-measures analysis of variance (ANOVA) with the between-subjects factor being the group and the butanol level as within-subjects factor. Age was included as a covariate. When a significant interaction factor was found we performed a repeated measures ANOVA for each group separately in order to explore linear trends. A planned contrast of the highest concentration condition minus the lowest concentration condition (β_{+2} vs β_{-1}) was also compared between groups when an interaction factor was identified. Since we had a strong prior hypothesis regarding group differences concerning OFC and PC, these analyses were only conducted in bilateral OFC (BA 11) and bilateral PC. A significance level α=0.05 was considered. When applicable, tests of sphericity were reported along with respective Greenhouse-Geisser corrections.

MVPA

Since classification procedures rely on the assumption of independent samples, a separate-subject GLM model with the same predictors as described above was performed which yielded beta estimates for each butanol level for each participant. Then 6 contrast maps (β_{-1} vs odorless air; β_0 vs odorless air; β_{+1} vs odorless air; β_{+2} vs odorless air; β_{+2} vs β_{-1}; β_{+2} + β_{+1} vs β_{-1} [1 1 -2]) were produced for each subject. All contrast maps were transformed to t-statistic maps in order to establish the same scaling across voxels for all participants.

Most disease-state classification studies have used support vector machine classifiers (SVM) (14-17) but logistic regression has already been successfully implemented in related brain decoding experiments (26). In this study a fast logistic regression classifier with L1-regularization was used as implemented in LIBLINEAR classification library (27). For each contrast, we used the t-statistic maps of all 53 subjects masked with the overall olfactory map as input to the classification analysis. Thus, each classification process included 53 independent samples with 317 features and 2 classes (controls and USH patients). A 20-fold stratified cross-validation scheme was used to assess the performance of our model by training and testing on separate subsets with approximately the same class proportions. Using the resulting confusion matrix, accuracy, sensitivity and specificity across folds were calculated. Decision values for each participant were used to calculate the area under curve (AUC) values. This process was repeated for each contrast. Significance was

evaluated with permutation testing (n=10000) for each model with random assignment of group class to the input t-statistic maps. The p-values were calculated with the resulting null-hypothesis distribution as the proportion of permutations that yielded greater accuracy than the accuracy obtained from each classification model. A significance level α=0.05 was considered.

RESULTS

ROIS UNIVARIATE ANALYSIS

In each ANOVA we first looked at the interaction effect between group and butanol level. Only if a non-significant interaction effect was found we evaluated the main effects. Whenever a factor was found to be statistically significant, proper posthoc analyses were run.

An interaction effect between group and butanol level was found in the right OFC (BA 11) ($F(2.365;118.247)=3.032$, $p=0.043$, Greenhouse-Geisser corrected, Mauchly's $W(5)=0.668$, $p=0.001$, $\varepsilon=0.788$) (Figure 2A). However, posthoc tests did not reveal significant differences between controls and USH patients for any butanol level (β_{-1}: $t(51)=0.162$, $p=0.872$; β_0: $t(51)=-0.861$, $p=0.393$; β_{+1}: $t(41.883)=0.313$, $p=0.756$; β_{+2}: $t(51)=-1.844$, $p=0.071$). In order to evaluate if there were differences between butanol concentration levels for each group we split the model and obtained non-significant butanol effect for both controls ($F(3;72)=0.979$, $p=0.408$) and USH patients ($F(2.195;54.872)=0.678$, $p=0.568$, Greenhouse-Geisser corrected, Mauchly's $W(5)=0.562$, $p=0.018$, $\varepsilon=0.732$). Separate repeated measures ANOVA showed a significant linear trend for controls, $F(1,25)=6.855$, $p=0.015$, but not for USH patients, $F(1,26)=0.413$, $p=0.526$.

Regarding the left OFC (BA 11), neither the interaction effect was significant ($F(3,150)=0.853$, $p=0.467$) nor the main effects of butanol ($F(3,150)=0.630$, $p=0.596$) and group ($F(1,50)=0.234$, $p=0.630$).

Also, an interaction effect between group and butanol level emerged in the right PC ($F(3,150)=4.537$, $p=0.004$) (Figure 2B). After this significant effect, posthoc analyses were run which did not reveal significant differences between USH patients and controls at Bonferroni corrected statistical significance $\alpha=0.05/4=0.0125$ (β_{-1}: $t(51)=0.718$, $p=0.476$; β_0: $t(51)=-0.941$, $p=0.351$; β_{+1}: $t(51)=-0.537$, $p=0.593$). Although not statistically significative, a marginal effect was found in the highest butanol concentration: β_{+2} ($t(51)=-2.342$, $p=0.023$. When we split the model to test the effect of butanol for each group separately only non-significant values arose (controls: $F(3;72)=2.333$, $p=0.081$; USH: $F(3;75)=1.934$, $p=0.131$). Separate repeated measures ANOVA showed a significant linear trend for USH patients, $F(1,26)=10.181$, $p=0.004$, but not for controls, $F(1,25)=1.760$, $p=0.197$.

In the left PC, interaction effect between group and butanol concentration proved to be non-significant ($F(2.453;125.113)=0.928$, $p=0.414$, Greenhouse-Geisser corrected, Mauchly's $W(5)=0.733$, $p=0.009$, $\varepsilon=0.818$). Furthermore, both main effects for butanol ($F(2.453;125.113)=0.702$, $p=0.525$, Greenhouse-Geisser corrected, Mauchly's $W(5)=0.733$, $p=0.009$, $\varepsilon=0.818$) and group ($F(1,51)=0.541$, $p=0.465$) were statistically non-significant.

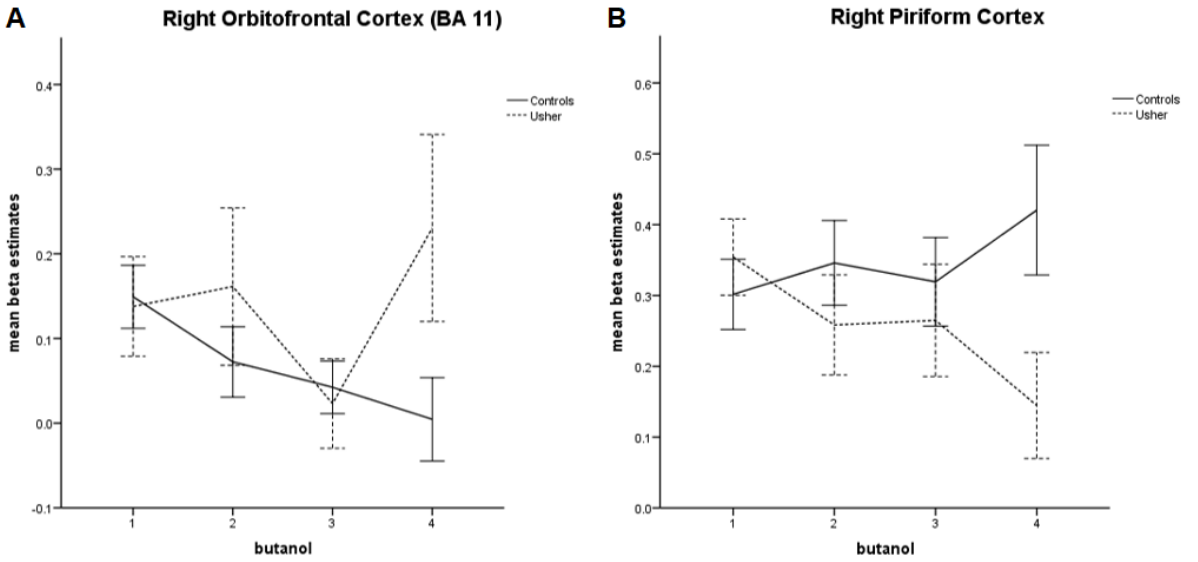

Figure 2: Interaction effect of group X butanol level: **A)** Controls show a decreasing response trend in right OFC (BA 11) when higher odorant concentrations are used. USH patients exhibit an inverse tendency (except for β_{+1}). **B)** There is an increasing response trend in controls when higher concentrations are used, and the opposite effect is seen in USH group. Group differences seem to be larger with higher odor concentrations. The bars display the standard error of the mean (SE).

Since butanol concentration presented to each participant during the fMRI task depended on individual olfactory thresholds it is also worth contrasting β_{+2} against β_{-1} and compare this contrast between groups. We hypothesized that this would provide a more reliable measure of the subject-specific variation of the stimulus-evoked response. This *a priori* defined contrast was only investigated in ROIs which showed a significant interaction factor. As for the right OFC (BA 11) we found a significant difference in this contrast between groups ($t(51)=2.339$, $p=0.023$) (Figure 3A). Also, a significant difference between USH patients and controls with respect to this contrast was revealed in the right PC ($t(51)=-3.380$, $p=0.001$) (Figure 3B).

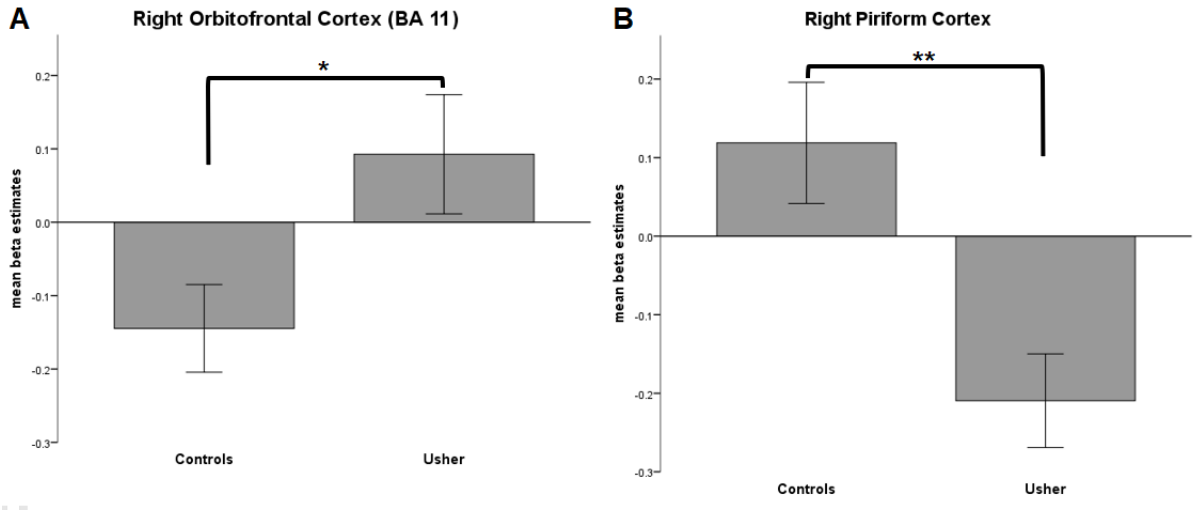

Figure 3: Planned contrast (β_{+2} vs β_{-1}) between USH patients and controls: **A)** USH group shows significantly higher response in the right OFC (BA 11). **B)** USH patients have significantly lower activity in the right piriform cortex. *p<0.05, **p<0.01. The bars display the standard error of the mean (SE).

MVPA ANALYSIS

The selected contrasts that were used as input to the classification analyses and the corresponding performance measurements are summarized in Table 2. The contrast β_{+2} + β_{+1} vs β_{-1} [1 1 -2] resulted in the best predictor model (accuracy=0.7170, p=0.0072; sensitivity=0.6774, p=0.0328; specificity=0.7727, p=0.0041; AUC=0.7849, p=0.0087). A graphical depiction of the classification performance for the best contrast (β_{+2} + β_{+1} vs β_{-1} [1 1 -2]) is shown in Figure 4.

Table 2: Performance measures for each contrast used as input to the classification analyses.

Contrasts	Accuracy	Sensitivity	Specificity	AUC
β_{-1} vs odorless air	**0.6604***	0.6429	**0.6800***	0.6681
β_{0} vs odorless air	0.5472	0.5313	0.5714	**0.6952***
β_{+1} vs odorless air	0.4340	0.4286	0.4400	0.3718
β_{+2} vs odorless air	0.4906	0.4815	0.5000	0.5641
β_{+2} vs β_{-1}	0.6226	0.6250	0.6207	0.6667
β_{+2} + β_{+1} vs β_{-1}	**0.7170****	**0.6774***	**0.7727****	**0.7849****

AUC=Area Under Curve. *p<0.05, **p<0.01.

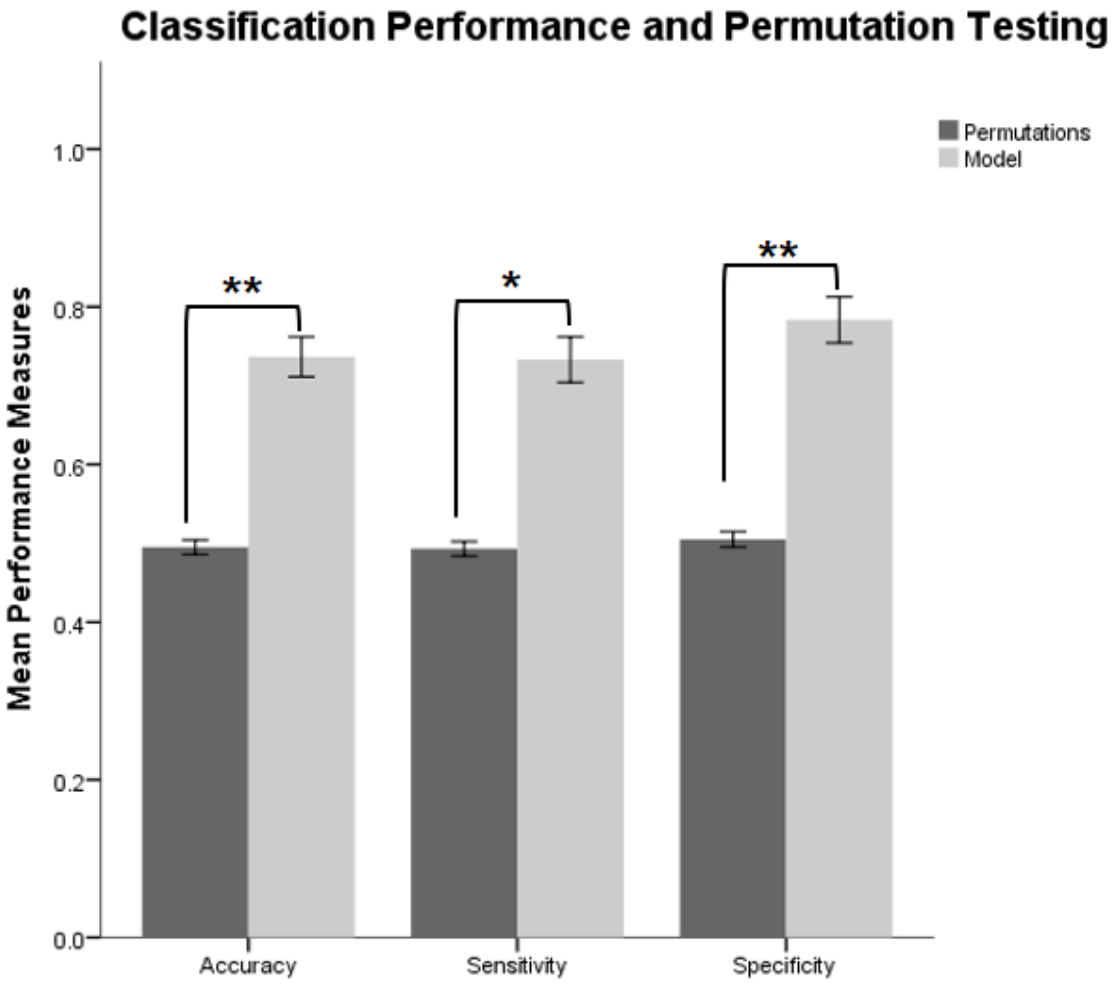

Figure 4: Performance measures for the best contrast model (β_{+2} + β_{+1} vs β_{-1} [1 1 -2]) and the corresponding measures yielded by the permutations testing. *p<0.05, **p<0.01. The bars display the standard error of the mean (SE) of the 20 folds of the model cross-validation and of the 10000 permutations.

DISCUSSION

This study aimed to shed new light on the effects of USH olfactory impairment in central olfactory brain regions. There are several studies in the literature reporting decreased olfactory function in USH patients although some results are conflicting (5, 28). Meanwhile, a more robust study has demonstrated that USH1 patients exhibit a faster ageing olfactory decline compared to controls (7). Besides USH, other ciliopathies such as Bardet-Biedl Syndrome have also been associated with olfactory dysfunction (29).

We compared stimulus-evoked responses between USH patients and healthy subjects within central olfactory regions in the context of an olfactory detection task. It should be noted that adapting the presented odorant concentrations during the fMRI task to each individual detection threshold is crucial in order to warrant the same difficulty across participants, compensate expected inter-subject variability and allow for a fair comparison across subjects.

Although the olfactory map retrieved from Neurosynth yielded other ROIs that could be investigated regarding group differences, we decided to restrict our univariate analyses to the OFC and PC. Wu et al. demonstrated that after a period of reduced odor input there is specifically a decrease in stimulus-evoked response in PC and the opposite occurs in OFC (13), which allowed to define a strong a priori hypothesis. Bearing this in mind we formulated the hypothesis that the most significant differences between groups would be verified in these areas. Also, we chose to perform the univariate analyses using specifically BA 11 in detriment of BA 47 as the former has been the OFC area mostly linked to olfactory processing (30). When it is possible to formulate strong hypothesis, these strategies avoid exploratory and underpowered statistical testing thus reducing false positives.

Overall, we found evidence for defective olfactory function in USH patients particularly in the right OFC and right PC. Repeated measures ANOVA revealed a significant interaction effect between group and butanol concentration for both right OFC and right PC. This means that differences between USH patients and healthy subjects are dependent upon odor concentration. Even though posthoc analyses with multiple comparisons correction failed to detect specific differences between groups for each butanol concentration, different trends in activation were clearly identified (Figure 2). One should note that posthoc tests are less sensitive to explore interactions than trend analysis. In fact, the observed interactions stem from the fact that controls showed a significant decreasing response trend in right OFC (Figure 2A) as higher odorant concentrations were used and USH patients exhibited an inverse tendency. The opposite scheme was verified in PC (Figure 2B) with controls increasing their response along higher intensity stimulus levels and USH patients showing significantly lower activation. The planned contrast (β_{+2} vs β_{-1}) showed that the mean

activation in the right OFC significantly increased from the infra-threshold to the higher odorant concentration in USH compared to controls (Figure 3A). On the contrary, in the right PC, the USH group exhibited a significant mean activation decline from the lowest to highest butanol concentration compared to controls (Figure 3B).

In healthy subjects PC activity seems to be relatively proportional to odor intensity which has been demonstrated in mice (31) and guinea pig (32) studies. On the other hand, OFC attempts to compensate for this putatively excessive input signal. In USH patients the opposite functional relation is verified in this study.

Previous studies have shown that hyposmia or anosmia conditions are associated with diminished activation in the PC (12,13) which is easily explained by the lack of information projecting from the second olfactory neuron. Since our results are consistent with those reports, they reinforce the notion of dysfunctional olfactory receptor cells in USH patients. Thus, it is natural to suppose that USH mutations must somehow affect olfactory neuroepithelium specifically in the nasal cilia. Interestingly, evidence for abnormal nasal cilia has been reported in 1979 in RP patients, some of them being USH patients (33). Further support to this hypothesis comes from a recent study which demonstrated the presence of USH proteins within the olfactory epithelium of mice and their interaction with olfactory signaling proteins (6).

The OFC is the high-order area that has been most linked with olfactory processing and its functions include odor quality discrimination and olfactory conscious awareness. Specifically, the right OFC plays a central role in conscious olfactory perception (34). It has been demonstrated that OFC volume is positively correlated with olfactory performance in respect to several tasks including odor sensitivity, odor quality discrimination and cued odor identification (35). Notably, a study found evidence of a decreasing stimulus-evoked response in PC after 7 days of olfactory deprivation whereas an increasing OFC activity was verified (13). These findings were explained as a compensatory mechanism that makes the olfactory system resistant to reversible derangements of afferent sensory input. Our data suggest that a similar process occurs in USH patients particularly for higher odor concentrations (Figure 2,3). However, in this case the olfactory deprivation is not transient but chronically progressive which is substantiated by USH patients faster age-related olfactory decline (7), suggesting that the type of acute adaptation observed in health participants is also observed chronically in patients.

It needs to be pointed out that only right-sided ROIs showed a significant interaction factor. The left PC ROI may have not showed this effect because it also contained a partial area of the left amygdala which may have caused a partial volume effect. However, that was not the case with the left OFC. In fact, evidence for dominant right OFC has been described

particularly with higher odor concentrations (36). Thus, it is possible that differences between groups are less relevant in the left side even when higher odor concentrations are used but not in the right side.

We demonstrated through an exploratory classification analysis that it is possible to predict weather a subject is an USH patient or a healthy individual based on the fMRI pattern of the olfactory network. MVPA procedures have been investigated as diagnostic tools in several neurological and psychiatric diseases that pose significant challenges in terms of diagnosis and classification (14-17). These studies have shown that specific regional fMRI patterns of activation carry discriminant information regarding the disease in study. Indeed, Chanel and colleagues reported an autism spectrum disorder categorization accuracy of 92.3% (14) while it has been reported a classification accuracy of 82.5% for social anxiety disorder (15) both using SVM classifiers. Although our results are not as promising as those, they still represent a significant classification model with 71.7% accuracy, 67.7% sensitivity and 77.2% specificity for the $\beta_{+2} + \beta_{+1}$ vs β_{-1} contrast using a logistic regression classifier with L1-regularization (Figure 4). This also indicates that discriminative information is contained within the olfactory network used in this analysis namely the OFC, PC, insula, amygdala and a small region that extended from the right OFC (BA 47) to the right temporal pole. We chose to run the classification analysis using all regions yielded by the meta-analysis based on the hypothesis that distributed alterations along several central olfactory regions occur in USH patients. Amygdala is considered part of the so-called primary olfactory cortex receiving direct axonal projections from the olfactory bulb (34) and insula is deeply involved in olfactory processing (37). Also, cortical thinning of the temporal pole has been associated with reductions in odor familiarity and cued odor matching (38). We only excluded the lateral globus pallidus to avoid biased classification based on potential movement differences between the two groups. It was not the purpose of this analysis to identify specific patterns within each olfactory region but to investigate whether distributed fMRI activity is potentially suited to identify USH patients.

Currently, USH diagnosis rely mostly on genetic testing although auditory, retinal and vestibular tests may narrow the differential diagnosis (39). Besides its clinical heterogeneity, USH is also characterized by genetically heterogeneity which is also present in each USH subtype (40). This means that some mutations can give rise to different clinical subtypes and even atypical USH (40). Therefore, it is necessary to improve both USH diagnosis and USH subtype categorization as each subtype exhibit different prognosis and require tailored management. The identification of fMRI biomarkers that can discriminate USH patients constitutes an attractive option as a screening test prior to definitive genetic testing. Also, it

could be used as an outcome measure in future therapeutic studies and eventually as a predictor of functional prognosis.

Our study was carried out with a small sample of USH patients (n=27) which limits the power of our statistical analysis. Larger series should be used to confirm our results and investigate other aspects such as putative correlations between fMRI central olfactory activation and psychophysical measures. Also, in this study we could not draw any conclusions regarding USH types because of small samples for USH1 (n=4) and USH3 (n=2) compared to USH2 (n=21) but this is of uttermost importance and should be addressed in future research. Other olfactory tasks such as olfactory discrimination and identification performed during fMRI could be helpful in better characterizing olfactory deficits. Further functional imaging studies should be conducted in order to identify olfactory-activated patterns that could elucidate the proposed compensatory mechanism and eventually be used as biomarkers of the disease. This requires both improved experimental conditions and better classification models. For instance, the classification performance would probably benefit from proper feature selection methods such as recursive feature elimination. Also, other classifiers might work better than the one we used in this study.

CONCLUSION

This study provides evidence of dysfunctional stimulus-evoked activation in the right PC and right OFC in USH patients through an olfactory task during fMRI. Furthermore, it shows that it is possible to discriminate patients and controls based on fMRI olfactory network patterns.

Further research is warranted with respect to putative differences between USH clinical types in central olfactory regions. This could provide insight to a better understanding of the mechanisms responsible for USH clinically heterogeneity. Also, a larger sample of USH patients should be studied in order to confirm our results and unveil possible effects that our analyses failed to detect due to lack of power. Detailed MVPA should be carried out aiming to elucidate the mechanisms underlying central olfactory regions dysfunction in USH patients.

ACKNOWLEDGEMENTS

I thank professor Miguel Castelo-Branco for giving me the opportunity to work in such a fascinating area as neuroscience and for the critical thinking regarding statistical analysis.

Also, I wish to thank Catarina Duarte for the willingness and patience she demonstrated while helping me in the process of learning functional imaging analysis.

Finally, I thank my family for all their support throughout the development of this project.

REFERENCES

1. Mathur P, Yang J. Usher syndrome: Hearing loss, retinal degeneration and associated abnormalities. Biochimica et biophysica acta. 2015;1852(3):406-20.

2. Kalloniatis M, Fletcher EL. Retinitis pigmentosa: understanding the clinical presentation, mechanisms and treatment options. Clinical & experimental optometry. 2004;87(2):65-80.

3. Frolenkov GI, Belyantseva IA, Friedman TB, Griffith AJ. Genetic insights into the morphogenesis of inner ear hair cells. Nature Reviews Genetics. 2004;5:489.

4. Millan JM, Aller E, Jaijo T, Blanco-Kelly F, Gimenez-Pardo A, Ayuso C. An update on the genetics of usher syndrome. Journal of ophthalmology. 2011;2011:417217.

5. Zrada SE, Braat K, Doty RL, Laties AM. Olfactory loss in Usher syndrome: another sensory deficit? American journal of medical genetics. 1996;64(4):602-3.

6. Jansen F, Kalbe B, Scholz P, Mikosz M, Wunderlich KA, Kurtenbach S, et al. Impact of the Usher syndrome on olfaction. Human molecular genetics. 2016;25(3):524-33.

7. Ribeiro JC, Oliveiros B, Pereira P, António N, Hummel T, Paiva A, et al. Accelerated age-related olfactory decline among type 1 Usher patients. Scientific Reports. 2016;6:28309.

8. Ramos JN, Ribeiro JC, Pereira AC, Ferreira S, Duarte IC, Castelo-Branco M. Evidence for impaired olfactory function and structural brain integrity in a disorder of ciliary function, Usher syndrome. NeuroImage: Clinical. 2019;22:101757.

9. Gottfried JA. Smell: central nervous processing. Advances in oto-rhino-laryngology. 2006;63:44-69.

10. Zald DH, Pardo JV. Functional neuroimaging of the olfactory system in humans. International journal of psychophysiology : official journal of the International Organization of Psychophysiology. 2000;36(2):165-81.

11. Henkin RI, Levy LM. Functional MRI of congenital hyposmia: brain activation to odors and imagination of odors and tastes. Journal of computer assisted tomography. 2002;26(1):39-61.

12. Iannilli E, Bitter T, Gudziol H, Burmeister HP, Mentzel HJ, Chopra AP, et al. Differences in anosmic and normosmic group in bimodal odorant perception: a functional-MRI study. Rhinology. 2011;49(4):458-63.

13. Wu KN, Tan BK, Howard JD, Conley DB, Gottfried JA. Olfactory input is critical for sustaining odor quality codes in human orbitofrontal cortex. Nature neuroscience. 2012;15(9):1313-9.

14. Chanel G, Pichon S, Conty L, Berthoz S, Chevallier C, Grèzes J. Classification of autistic individuals and controls using cross-task characterization of fMRI activity. NeuroImage: Clinical. 2016;10:78-88.

15. Frick A, Gingnell M, Marquand AF, Howner K, Fischer H, Kristiansson M, et al. Classifying social anxiety disorder using multivoxel pattern analyses of brain function and structure. Behavioural brain research. 2014;259:330-5.

16. Koch SP, Hagele C, Haynes JD, Heinz A, Schlagenhauf F, Sterzer P. Diagnostic classification of schizophrenia patients on the basis of regional reward-related FMRI signal patterns. PloS one. 2015;10(3):e0119089.

17. Bhaumik R, Jenkins LM, Gowins JR, Jacobs RH, Barba A, Bhaumik DK, et al. Multivariate pattern analysis strategies in detection of remitted major depressive disorder using resting state functional connectivity. NeuroImage: Clinical. 2017;16:390-8.

18. Smith RJ, Berlin CI, Hejtmancik JF, Keats BJ, Kimberling WJ, Lewis RA, et al. Clinical diagnosis of the Usher syndromes. Usher Syndrome Consortium. American journal of medical genetics. 1994;50(1):32-8.

19. Hayes JE, Jinks AL. Evaluation of smoking on olfactory thresholds of phenyl ethyl alcohol and n-butanol. Physiology & behavior. 2012;107(2):177-80.

20. Freitas S, Simoes MR, Alves L, Santana I. Montreal Cognitive Assessment (MoCA): normative study for the Portuguese population. Journal of clinical and experimental neuropsychology. 2011;33(9):989-96.

21. Tabert MH, Steffener J, Albers MW, Kern DW, Michael M, Tang H, et al. Validation and optimization of statistical approaches for modeling odorant-induced fMRI signal changes in olfactory-related brain areas. NeuroImage. 2007;34(4):1375-90.

22. Croy I, Lange K, Krone F, Negoias S, Seo HS, Hummel T. Comparison between odor thresholds for phenyl ethyl alcohol and butanol. Chemical senses. 2009;34(6):523-7.

23. Yarkoni T, Poldrack RA, Nichols TE, Van Essen DC, Wager TD. Large-scale automated synthesis of human functional neuroimaging data. Nature methods. 2011;8(8):665-70.

24. Thye MD, Murdaugh DL, Kana RK. Brain Mechanisms Underlying Reading the Mind from Eyes, Voice, and Actions. Neuroscience. 2018;374:172-86.

25. Fuentes-Claramonte P, Martin-Subero M, Salgado-Pineda P, Alonso-Lana S, Moreno-Alcazar A, Argila-Plaza I. Shared and differential default-mode related patterns of activity in an autobiographical, a self-referential and an attentional task. 2019;14(1):e0209376.

26. Brown TI, Carr VA, LaRocque KF, Favila SE, Gordon AM, Bowles B, et al. Prospective representation of navigational goals in the human hippocampus. Science (New York, NY). 2016;352(6291):1323-6.

27. Fan R-E, Chang K-W, Hsieh C-J, Wang X-R, Lin C-J. LIBLINEAR: A Library for Large Linear Classification. J Mach Learn Res. 2008;9:1871-4.

28. Seeliger M, Pfister M, Gendo K, Paasch S, Apfelstedt-Sylla E, Plinkert P, et al. Comparative study of visual, auditory, and olfactory function in Usher syndrome. Graefe's archive for clinical and experimental ophthalmology = Albrecht von Graefes Archiv fur klinische und experimentelle Ophthalmologie. 1999;237(4):301-7.

29. Braun JJ, Noblet V, Durand M, Scheidecker S, Zinetti-Bertschy A, Foucher J, et al. Olfaction evaluation and correlation with brain atrophy in Bardet-Biedl syndrome. Clinical genetics. 2014;86(6):521-9.

30. Kringelbach ML, Rolls ET. The functional neuroanatomy of the human orbitofrontal cortex: evidence from neuroimaging and neuropsychology. Progress in neurobiology. 2004;72(5):341-72.

31. Stettler DD, Axel R. Representations of Odor in the Piriform Cortex. Neuron. 2009;63(6):854-64.

32. Sugai T, Miyazawa T, Fukuda M, Yoshimura H, Onoda N. Odor-concentration coding in the guinea-pig piriform cortex. Neuroscience. 2005;130(3):769-81.

33. Arden GB, Fox B. Increased incidence of abnormal nasal cilia in patients with retinitis pigmentosa. Nature. 1979;279(5713):534-6.

34. Gottfried JA. Central mechanisms of odour object perception. Nature reviews Neuroscience. 2010;11(9):628-41.

35. Seubert J, Freiherr J, Frasnelli J, Hummel T, Lundstrom JN. Orbitofrontal cortex and olfactory bulb volume predict distinct aspects of olfactory performance in healthy subjects. Cerebral cortex (New York, NY : 1991). 2013;23(10):2448-56.

36. Sobel N, Prabhakaran V, Hartley CA, Desmond JE, Glover GH, Sullivan EV, et al. Blind smell: brain activation induced by an undetected air-borne chemical. Brain : a journal of neurology. 1999;122 (Pt 2):209-17.

37. Frasnelli J, Lundstrom JN, Boyle JA, Djordjevic J, Zatorre RJ, Jones-Gotman M. Neuroanatomical correlates of olfactory performance. Experimental brain research. 2010;201(1):1-11.

38. Olofsson JK, Rogalski E, Harrison T, Mesulam MM, Gottfried JA. A cortical pathway to olfactory naming: evidence from primary progressive aphasia. Brain : a journal of neurology. 2013;136(Pt 4):1245-59.

39. Bonnet C, El-Amraoui A. Usher syndrome (sensorineural deafness and retinitis pigmentosa): pathogenesis, molecular diagnosis and therapeutic approaches. Current opinion in neurology. 2012;25(1):42-9.

40. Yan D, Liu XZ. Genetics and pathological mechanisms of Usher syndrome. Journal of human genetics. 2010;55(6):327-35.